TISSUE ENGINEERING: Part A
Volume 17, Numbers 13 and 14, 2011

DOI: 10.1089/ten.tea.2010.0446

Improving Bone Formation in a Rat Femur Segmental Defect by Controlling Bone Morphogenetic Protein-2 Release

Kate V. Brown, MRCS (Lon),[1] Bing Li, Ph.D.,[2,*] Teja Guda, Ph.D.,[1,3] Daniel S. Perrien, Ph.D.,[4] Scott A. Guelcher, Ph.D.,[2] and Joseph C. Wenke, Ph.D.[1]

Nonunion is a common complication in open fractures and other severe bone injuries. Recombinant human bone morphogenetic protein-2 (rhBMP-2) delivered on a collagen sponge enhances healing of fractures. However, the burst release of rhBMP-2 necessitates supra-physiological doses of rhBMP-2 to achieve a robust osteogenic effect, which introduces risk of ectopic bone formation and severe inflammation and increases the cost. Although the concept that the ideal pharmacokinetics for rhBMP-2 includes both a burst and sustained release is generally accepted, investigations into the effects of the release kinetics on new bone formation are limited. In the present study, biodegradable polyurethane (PUR) and PUR/microsphere [PUR/poly(lactic-*co*-glycolic acid)] composite scaffolds with varying rhBMP-2 release kinetics were compared to the collagen sponge delivery system in a critical-sized rat segmental defect model. Microcomputed tomography analysis indicated that a burst followed by a sustained release of rhBMP-2 from the PUR scaffolds regenerated 50% more new bone than the collagen sponge loaded with rhBMP-2, whereas a sustained release without the burst did not form significantly more bone than the scaffold without rhBMP-2. This study demonstrated that the putative optimal release profile (i.e., burst followed by sustained release) for rhBMP-2 can be achieved using PUR scaffolds, and that this enhanced pharmacokinetics regenerated more bone than the clinically available standard of care in a critical-sized defect in rat femora.

Introduction

Nonunion complicates many bone defects, and has an incidence rate up to 32% in severe lower extremity injuries.[1] To avoid nonunions, conventional management typically involves bone grafting or lengthening procedures, but these approaches have significant drawbacks such as donor-site morbidity, infection, and prolonged rehabilitation. More recently, bone has been successfully regenerated using osteogenic factors such as recombinant human (rh) bone morphogenetic proteins (BMPs).[2–8] rhBMPs have a profound osteogenic effect due to several different mechanisms, such as osteoinduction,[9] promotion of cell growth and differentiation,[10] and recruitment of osteoprogenitor cells essential for bone development, remodeling, and repair.[11]

Incorporation of growth factors into scaffolds and delivery systems is a rapidly expanding area of research in tissue engineering. rhBMP-2 delivered on a collagen sponge (INFUSE® Bone Graft; Medtronic) has been approved by FDA for posterior-lateral spine fusions, tibial fractures, and sinus and alveolar ridge augmentations. The collagen sponge rapidly releases the rhBMP-2,[12,13] which has been suggested to initiate the osteogenic cascade by recruitment of osteoprogenitor cells.[14] Due to this bolus release, rhBMP-2 rapidly diffuses away from the fracture site before achieving a critical density of newly infiltrated cells,[13] thereby necessitating supra-physiological doses of rhBMP-2 for a robust osteogenic affect with an accompanying risk of ectopic bone formation and severe inflammation in clinical practice.[7,8] Further, rapid release of rhBMP has been reported to result in transient osteoclast-mediated resorption before new bone formation in metaphyseal defects.[13–15] These observations have led to suggestions that the use of a single protein may be too simplistic an approach,[16] which are supported by a recent study showing that dual delivery of rh-vascular endothelial growth factor and rhBMP-2 synergistically enhanced bone regeneration relative to either factor alone.[17,18] There is evidence suggesting that a sustained delivery of rhBMP-2 enhances bone regeneration, which has been attributed to its effect on a larger

The work was performed at Vanderbilt University and the U.S. Army Institute of Surgical Research.
[1]Extremity Trauma and Regenerative Medicine Task Area, United States Army Institute of Surgical Research, San Antonio, Texas.
[2]Department of Chemical and Biomolecular Engineering, Vanderbilt University, Nashville, Tennessee.
[3]Wake Forest Institute of Regenerative Medicine, Winston-Salem, North Carolina.
[4]Department of Orthopaedics and Rehabilitation and Center for Bone Biology, Vanderbilt University, Nashville, Tennessee.
*Current affiliation: GE Global Research Center, One Research Circle, Niskayuna, New York.

Report Documentation Page

Form Approved
OMB No. 0704-0188

1. REPORT DATE	2. REPORT TYPE	3. DATES COVERED
01 JUL 2011	**N/A**	**-**

4. TITLE AND SUBTITLE	5a. CONTRACT NUMBER
Improving bone formation in a rat femur segmental defect by controlling bone morphogenetic protein-2 release	5b. GRANT NUMBER
	5c. PROGRAM ELEMENT NUMBER
6. AUTHOR(S)	5d. PROJECT NUMBER
Brown K. V., Li B., Guda T., Perrien D. S., Guelcher S. A., Wenke J. C.,	5e. TASK NUMBER
	5f. WORK UNIT NUMBER
7. PERFORMING ORGANIZATION NAME(S) AND ADDRESS(ES)	8. PERFORMING ORGANIZATION REPORT NUMBER
United States Army Institute of Surgical Research, JBSA Fort Sam Houston, TX	
9. SPONSORING/MONITORING AGENCY NAME(S) AND ADDRESS(ES)	10. SPONSOR/MONITOR'S ACRONYM(S)
	11. SPONSOR/MONITOR'S REPORT NUMBER(S)

12. DISTRIBUTION/AVAILABILITY STATEMENT
Approved for public release, distribution unlimited

13. SUPPLEMENTARY NOTES

14. ABSTRACT

15. SUBJECT TERMS

16. SECURITY CLASSIFICATION OF:			17. LIMITATION OF ABSTRACT	18. NUMBER OF PAGES	19a. NAME OF RESPONSIBLE PERSON
a. REPORT	b. ABSTRACT	c. THIS PAGE			
unclassified	**unclassified**	**unclassified**	**UU**	**12**	

population of osteoprogenitor cells at the fracture site at later stages following the original injury,[19–21] as well as its role in promoting vasculogenesis.[22] The development of improved delivery systems for rhBMP-2 has been reviewed[13,23–25] and is an active area of research.

Biodegradable polyurethane (PUR) scaffolds have been investigated as delivery systems for growth factors[26–28] and antibiotics[29,30] and present several advantages. PURs are biocompatible, moderately osteoconductive polymers that biodegrade to noncytotoxic breakdown products *in vivo*.[28,31–34] They can be injected into bony defects as a two-component liquid system, which cures *in situ* to form a solid scaffold with tough mechanical properties and preexisting, interconnected pores.[35] Further, the rate of degradation can be controlled by the choice of intermediates used in the synthesis of the scaffold.[28,36] In our previous study investigating the effects of rhBMP-2 release kinetics on bone regeneration in a rat femoral plug model, the addition of rhBMP-2 to the PUR scaffolds predictably resulted in more bone formation than the blank scaffolds.[37] In addition, scaffolds that had both a burst and sustained release of rhBMP-2 promoted significantly more new bone formation than those that only had a sustained release. This observation was attributed to the burst release of rhBMP-2 enhancing the recruitment and condensation of osteoprogenitor cells into the scaffold.

Our previous study demonstrated that rhBMP-2 release kinetics from PUR scaffolds affected the volume of bone regenerated in a non-critical-sized femoral plug defect, and that both a burst and a sustained release are beneficial.[37] Although the notion that the ideal pharmacokinetics comprises both a burst and a sustained release is largely accepted, investigations into the effects of the release kinetics on new bone formation are limited,[25] and some studies have not shown significant differences in new bone formation with varying release kinetics.[23,38] Further, although the limitations of the collagen sponge as a carrier for rhBMP-2 have been well documented, there is a paucity of evidence demonstrating that other delivery systems with tunable release kinetics actually regenerate more bone in an osseous defect. Considering the limitations of the self-healing plug defect model, in the present study we investigated the effects of rhBMP-2 release kinetics from PUR and PUR/microsphere composite scaffolds on new bone formation in more challenging critical-sized segmental defects in rat femora. The objective of the study was to compare new bone formation in the PUR scaffolds with tunable release kinetics to that of the clinical standard of care (collagen sponge).

Methods

Experimental design

A previously described rat femoral critical-sized segmental defect model (with a length of 6 mm)[4] was used to investigate the difference in bone regeneration between rhBMP-2 delivered from a collagen sponge or from Slow or Fast Release (SR or FR) PUR scaffolds over a 4- or 8-week time period. The rats were divided into five groups with two time points ($n=10$): Collagen sponge and rhBMP-2 (collagen + BMP), FR scaffolds and rhBMP-2 (FR + BMP), SR scaffolds and rhBMP-2 (SR + BMP), blank FR scaffolds, and blank SR scaffolds. The study design is summarized in Table 1.

Table 1. Study Design for the Critical-Sized Segmental Defects in Rat Femora

Treatment group	*Nomenclature*	*4 weeks*	*8 weeks*
Collagen + rhBMP-2	Collagen + BMP	10	10
Fast release PUR scaffolds + rhBMP-2	FR + BMP	10	10
Slow release PUR scaffolds + rhBMP-2	SR + BMP	10	10
Blank fast release PUR scaffolds	FR	10	10
Blank slow release PUR scaffolds	SR	10	10

PUR, polyurethane; rhBMP-2, recombinant human bone morphogenetic protein-2.

Materials preparation

The bovine microfibullar collagen I absorbable collagen sponge (MedChem Products, Inc.)[39] was cut under sterile conditions into 6 × 3 × 2 mm implants, each loaded with 2 μg rhBMP-2 (RD Systems®) in solution for 15 min before implantation. PUR and PUR/microsphere composite scaffolds were prepared as reported previously[37] from a two-component reaction between lysine triisocyanate (LTI) and a resin containing a polyester triol (polyol), water, catalyst, pore opener, and stabilizer. The polyol (900 Da) was prepared from a glycerol starter and a backbone comprising 70wt% ε-caprolactone, 20wt% glycolide, and 10wt% D,L-lactide as published previously.[11,13] The blank FR scaffolds had no further modifications. For the FR scaffolds with rhBMP-2 (FR + BMP, a burst followed by a sustained release), lyophilized rhBMP-2 powder (60:20:1 glucose:heparin:rhBMP-2) was encapsulated within the scaffold walls in a uniformly distributed manner by mixing the powder with the resin before reacting with LTI. The targeted index (the ratio of NCO to OH equivalents × 100) was 115 for FR and FR + BMP scaffolds.

To prepare PUR/microsphere composite scaffolds, the poly(lactic-*co*-glycolic acid) (PLGA) microspheres were first prepared from a double emulsion (water-oil-water) technique with or without rhBMP-2 in the first water phase as described previously.[37] PLGA (50/50, 0.58 dL/g) and PEG (4600 Da), at a ratio of 9:1, were dissolved in DCM at polymer concentrations of 5%. A glucose solution of rhBMP-2 was added to the polymer DCM solution, followed by sonication to form the water-in-oil emulsion. The water-in-oil emulsion was then added to a 5% PVA solution and a homogenizer was used for the first 100 s of stirring. Subsequently, the double emulsion was mixed using a stir bar for another 2.5 h to evaporate the DCM solvent. The particle size distribution was determined by dynamic laser light scattering (Malvern ZetaSizer 3000HS), and the spherical particle morphology was confirmed by SEM.[37] For the blank SR scaffolds, blank PLGA microspheres were mixed with resin before reaction with LTI. For the SR scaffolds with rhBMP-2 (SR + BMP, a sustained release with no burst), PLGA microspheres encapsulated with rhBMP-2 were mixed with resin before the reaction with LTI. The targeted index (the ratio of NCO to OH equivalents × 100) was 100 for SR and SR + BMP scaffolds. All implants were 6 × 3 mm cylindrical pieces, and each implant contained 2 μg rhBMP-2 (47 μg/mL). Pore size and internal pore morphology

of the PUR scaffolds were determined using scanning electron microscopy (Hitachi S-4200 SEM).

In vitro *release experiment*

Three replicates of the PUR scaffolds or collagen sponge (~50 mg) containing rhBMP-2 were immersed in 1 mL release medium (α-MEM containing 1% BSA) contained in polypropylene vials sealed by O-rings. BSA was included to minimize adsorption of growth factors onto the implants and vials,[27,37] and the medium was refreshed every 24 h. Daily release was determined using a Human BMP-2 Quantikine ELISA kit (R&D Systems).

Surgical procedures

This study has been conducted in compliance with the Animal Welfare Act, the Implementing Animal Welfare Regulations and in accordance with the principles of the Guide for the Care and Use of Laboratory Animals.

The methods used for the critical-sized defect creation and fixation are described previously.[5] Briefly, a 6-mm segmental defect was created and stabilized in the left femur of 100 adult male Sprague-Dawley rats (Harlan; average weight 391 + 11 g, range 354–416 g). Using aseptic technique, a longitudinal incision was made, and the entire femoral shaft was exposed using blunt dissection. A polyacetyl plate was fixed to the surface of the femur using threaded K-wires. A 6-mm mid-diaphyseal full-thickness defect was created with a reciprocating saw under continuous irrigation with saline. The defects in all animals were implanted either with a BMP-soaked collagen sponge implant or the designated PUR scaffold for that experimental group (see above). The wound was closed in a layered fashion. A high-resolution radiograph of each femur with the stabilized defect was obtained using a Faxitron X-ray system (Faxitron X-ray Corporation [Model: MX-20] Image settings Time: 15 Sec KV: 35 Window Level: 3380/1250) after initial surgery to confirm proper surgical technique and fixation. The animals were allowed full activity in their cages postoperatively, administered adequate analgesia (buprenorphine), and monitored daily for signs of pain and infection. The animals were euthanized 4 or 8 weeks later with Fatal Plus, and the femurs were harvested and immersed in formalin for 48 h and then 70% alcohol for further assessment.

Outcomes assessment: Microcomputed tomography

The samples were scanned using microcomputed tomography (microCT) SkyScan 1076 (Skyscan) at 100 kV source voltage and 100 μA source current with no filter used and at a spatial resolution of 8.77 μm. The reconstructions were performed using NRecon software (Skyscan) and resulted in grayscale images that spanned a density range from 960 to 2570 mg/cm^3 corresponding to gray-scale values 0–255. DataViewer (Skyscan) was used to reslice the microCT images along coronal sections that were used to reorient the microCT slices to be perpendicular to the axis of the femurs and microCT thresholding was performed to include only ossified tissues. The thresholds were selected as the histogram minima between the peaks representing the formalin in which the sample was scanned and the mineralized bone volume (BV) of the sample. The geometric mean of the threshold for all 100 samples in the study was used to determine the threshold for separation of the mineralized tissue from poorly mineralized tissue as 39, which corresponds to a density of 1200 mg/cm^3. This global threshold for mineralized tissue recognition is equivalent to 40.3% of mature cortical attenuation of the femoral cortex that is between the 2nd and 3rd K-wires away from the diaphyseal defect and compares well to other mineralized callus identification techniques.[40] The tissue mineral density (TMD) was computed as the weighted mineral density of all the voxels above the mineralization threshold.

The region of interest (ROI) was registered in each sample by selecting the first microCT axial section of the femur above and below the defect in which the K-wire was visible and then selecting the midpoint of this span to be the central slice of the 6 mm defect created in the femoral diaphysis. The extent of the volume of interest was thus determined as spanning between the axial sections 3 mm above (physiologically proximal) and below (distal) this midpoint and these are referred to as the defect interfaces for the purposes of the microCT analysis (Fig. 4A). Within the axial cross section, the periphery of the mineralized tissue that showed three-dimensional connectivity was manually selected every 440 μm (50 axial slices) and interpolated in between to generate a volume of interest called the callus volume (CV) (Fig. 4B) to evaluate differences in tissue mineralization between the groups that demonstrated bridging of the defect. Within these groups, the mineralized tissue volume was also calculated for each 8.77 μm slice from the distal to the proximal interface along the 6 mm defect span to evaluate differences in the tissue mineralization patterns across carriers. To investigate the ability of the mineralized tissue callus to maintain space within the femoral defect created, a femur defect volume (DV) of interest (Fig. 4C) was determined by adaptively interpolating the periphery of the femur selected 880 μm outside both defect interfaces. The BV was computed using CTAn software (Skyscan) both within the CV as well as within the 6 mm defect span but unconnected to the mineralization within the CV. The ratio of the CV to the DV was used to evaluate the efficacy of the carrier to function as a space maintainer.

Outcomes assessment: Histology

Specimens were fixed in 10% Neutral Buffered Formalin for 2 weeks, dehydrated, infiltrated, and embedded in methylmethacrylate. Five-μm-thick central sections were cut in the longitudinal plain and stained with modified Goldner's trichrome[41] to differentiate between bone/soft tissue and polymer: mineralized tissue stained dark green, osteoid and collagen bright red, soft tissue pink to light green, and erythrocytes bright orange. In specimens containing polymer, the polymer appears as unstained white area within the defect. For quantitative analysis of the relative areas of bone, soft tissue, and polymer, high-resolution digital images were acquired at 1.25× or 20×. The area of interest comprising the bone defect area was defined by drawing a quadrilateral area using the periosteal corners of the four host cortices as points of reference. The relative areas of bone, soft tissue, and polymer (when present) within the defect were quantified using Metamorph software (Molecular Devices, Inc.) and were calculated and reported as a percentage of the ROI. By reporting all data as a percentage or proportion of the total

ROI area (e.g., % Bone, % Soft Tissue) the data are normalized and to individual section and cancels variance caused by slight differences in defect length, width or angle that occur as an artifact of 2D sectioning.

Statistics

All data were analyzed using SAS 9.1. Descriptive statistics included mean, standard deviation, median, and interquartile ranges. Data from the 4-week time point was compared to the 8-week time point using a Student's *t*-test for parametric data and a Wilcoxon Two-Sample Test for nonparametric data. Treatment groups were compared within each week using an ANOVA and a Tukey's HSD test for *post hoc* pair wise comparisons. Statistical significance was set at $p < 0.05$.

Results

Synthesis and characterization of the PUR scaffolds and PLGA microspheres

The pore size and morphology of FR and SR scaffolds were similar to values previously reported for PUR scaffolds synthesized from LTI and hexamethylene diisocyanate trimer.[37] The porosity and mean pore size of the FR scaffolds were 93.4% and 245 ± 45 μm, respectively. The SR scaffolds, which had the incorporation of 1.3 μm PLGA microspheres, had a porosity of 89.6% and pore size of 334 ± 129 μm. These results are consistent with our previous study[37] demonstrating that the PLGA microspheres did not substantially change the morphology of the PUR scaffolds.

In vitro *release profile of rhBMP-2 from collagen carrier and PUR scaffolds*

The *in vitro* release kinetics for the collagen, FR + BMP, and SR + BMP scaffolds are shown in Figure 1. The cumulative release of rhBMP-2 from the collagen carrier was 92% on day 1 and reached 100% on day 2 (Fig. 1A). When rhBMP-2 was embedded into the scaffold walls as a lyophilized powder (FR + BMP), a burst release of 36% was observed on day 1. By day 4, a total of 58% of the drug had been released, and a period of sustained release until day 21 for a cumulative release of 71%. In contrast, when rhBMP-2 was encapsulated in PLGA microspheres (1.3 μm) before incorporation into the PUR scaffold, the burst release was nearly eliminated (~3% on day 1), but the sustained release period (from day 5 to 21) is similar to that of the FR + BMP. The SR + BMP released 22% of the BMP in 21 days. The daily release plots (Fig. 1B) show that the release of rhBMP-2 from the collagen sponge was <1 ng/mL by day 3. Interestingly, although the concentration of rhBMP-2 released from FR + BMP scaffolds was an order of magnitude higher than that release from SR + BMP scaffolds from days 1–4, by day 5 the daily release from both scaffolds was nearly identical. Therefore, the FR + BMP and SR + BMP delivery systems, by design, exhibit release kinetics that are the same except for the burst release observed during the first 4 days.

In vivo *study of rhBMP-2 scaffolds and collagen implants in rat femoral critical-sized defects*

There were no animals excluded from our analysis or complications in the *in vivo* experiment. Rats gained an average of 2% and 15% in weight from surgery to necropsy at 4 and 8 weeks, respectively. MicroCT analysis demonstrated that significantly more new bone ($p < 0.001$) was regenerated in the FR + BMP group compared to all of the other groups at the 4- and the 8-week time points (Fig. 2A). The collagen + BMP group regenerated significantly more bone ($p < 0.001$) than the SR, FR, and SR + BMP groups. Surprisingly, the SR + BMP group did not promote more new bone formation than either the SR or FR groups without rhBMP-2. In addition, there were no significant increases ($p = 0.124$) in the amount of total bone regenerated at the 4-week time point compared to the 8-week time point in any group. There was a significant increase in bone density ($p < 0.001$) between 4 and 8 weeks for all the treatment groups. In addition, bone density in the FR + BMP treatment group was significantly less ($p = 0.02$) than the other four treatment groups (Fig. 2B). Representative microCT images (Fig. 3) illustrate these findings. Bridging of the defect was observed at both 4 and 8 weeks in all samples in the collagen + BMP and FR + BMP

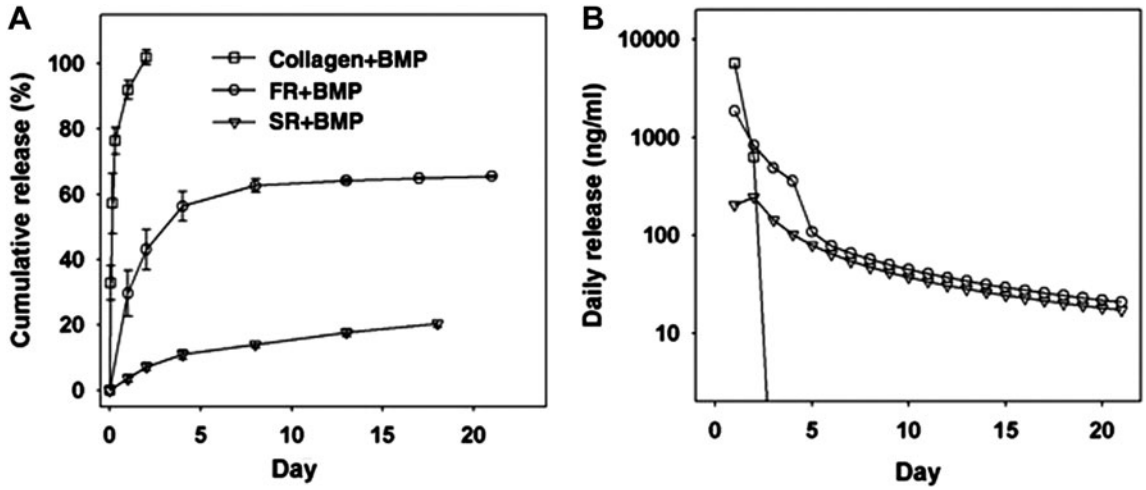

FIG. 1. *In vitro* release kinetics for recombinant human bone morphogenetic protein (BMP)-2 released from FR + BMP and SR + BMP scaffolds and the collagen sponge. **(A)** Cumulative release. **(B)** Daily release. FR, fast release; SR, slow release.

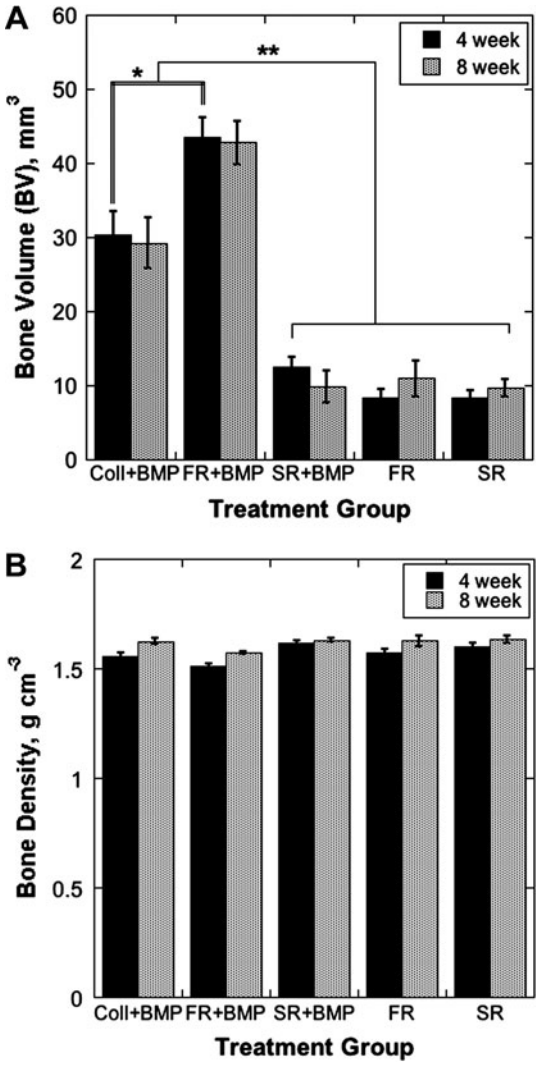

FIG. 2. Analysis of new bone formation as measured by microcomputed tomography (microCT). **(A)** Bone volume. Collagen + BMP and FR + BMP were significantly higher than the other at 4 and 8 weeks. FR + BMP had significantly more bone than collagen + BMP at both time periods. $*p < 0.001$; $**p < 0.001$. **(B)** Bone density. All groups significantly increased density between 4 and 8 weeks. FR + BMP was significantly less than all other groups at 4 and 8 weeks.

groups. It was observed (Fig. 4D) that the ossified callus maintained a significantly greater volume of the original bone defect open in the FR + BMP group (79%) at both 4 ($p < 0.001$) and 8 weeks ($p = 0.001$) when compared to the collagen + BMP group (49%). In addition, the distribution of bone volume within the callus (BV/CV) was also significantly denser in the collagen + BMP group at 4 weeks than the FR + BMP group ($p < 0.001$), whereas no significant differences ($p = 0.12$) were observed at 8 weeks between groups (Fig. 4E). When the bone regenerated along the length of the 6 mm was evaluated for the collagen + BMP and FR + BMP groups at 4 and 8 weeks, it was observed that the FR + BMP group showed more bone at all locations within the defect at both 4 and 8 weeks (Fig. 5).

Representative histological sections cut from each of the BMP-treated groups are shown in Figure 6. In the 4-week samples, the PUR scaffolds are still visible, but the collagen carrier has been degraded. There is inconsistent bone formation in the collagen + BMP sample within the defect, some in continuity with the host cortex as well as some marrow infiltration and scattered blood vessels. In addition, many of the collagen + BMP samples showed substantial prolapse of skeletal muscle into the defect area. Both the SR and FR blank scaffolds and SR + BMP groups show polymer with some marrow, skeletal muscle, and fibrous tissue infiltration into the pores, but blunted callus formation at both ends of the defect. The FR + BMP scaffolds show osteoid formation within the callus along the longitudinal axis in line with host cortex. On higher magnification, within the scaffold architecture there is a remarkably consistent pore tissue pattern with concentric rings of large blood vessels at the pore edge surrounding new bone with osteoid on the inner edge and/or outer surface, which in many cases surrounded new marrow at the center of the pore (Fig. 7). Smaller blood vessels were consistently found throughout inner volume of the pores. This pattern was very consistent throughout the FR + BMP group and was not seen in any specimens from other treatment groups.

At 8 weeks, considerable organized mineralized bone had formed in the FR + BMP samples. The representative histological section of an FR + BMP scaffold in Figure 8 (the approximate boundary of the implant is denoted by the box) shows a mature and fully bridged periosteal callus, which was observed in 4 out of 10 FR + BMP scaffolds compared to 1 out of 10 in the collagen + BMP treatment group (not statistically significant, $p = 0.3$). This trend is in agreement with the microCT images showing more new periosteal bone formation and bridging at the cortexes in the FR + BMP group. The collagen + BMP also showed mineralized periosteal and endosteal bone formation. Mineralized new bone in the remaining three groups was only observed at the ends of the defect and bridging did not occur.

In agreement with the microCT results, there was significantly more mineralized bone ($p < 0.002$) in the collagen + BMP and FR + BMP samples at both the 4- and the 8-week time points versus all other groups as measured by histomorphometry. However, there was no significant difference in the amount of new bone formation in the FR + BMP scaffolds compared to collagen + BMP scaffolds at either time point ($p > 0.9$) (Fig. 9A). The amount of PUR remaining in the FR and FR + BMP scaffolds at 4 and 8 weeks as measured by histomorphometry is plotted in Figure 9B. The PUR component in the FR scaffolds was 60 area% at week 4 and 42 area% at week 8, compared to 51 area% at week 4 and 46 area% at week 8 for FR + BMP scaffolds. While the PUR component decreased from week 4 to 8 for both treatment groups, the reduction in PUR area% with time was significant only in the FR group ($p < 0.001$). Further, the difference in PUR area% between the FR and FR + BMP scaffolds at each time point was not significant ($p = 0.764$).

Discussion

The osteogenic potential of PUR scaffolds incorporating rhBMP-2 with two different release strategies was compared to that of the collagen sponge delivery system in critical-sized segmental defects in rat femora. Considering a previous study showing that critical-sized defects treated with an empty collagen sponge treatment with rhBMP-2 do

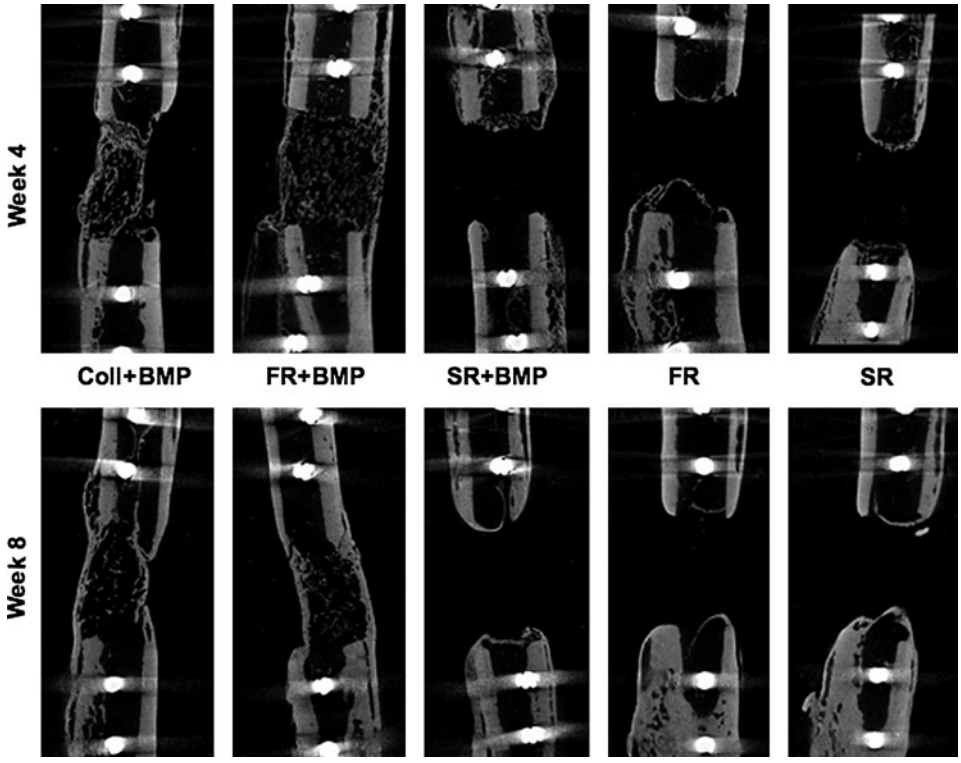

FIG. 3. Representative microCT images of new bone formation (all images are scaled from 18 mm in length along the longitudinal axis). Coll, collagen.

not support new bone formation,[42] an empty collagen sponge was not included in the study design. At both 4 and 8 weeks, microCT analysis demonstrated that the PUR scaffold characterized by a burst followed by a sustained release (denoted FR + BMP) formed ~50% more bone than the collagen + BMP. In contrast, the amount of new bone formed in the PUR scaffold with only a sustained release of rhBMP-2 (SR + BMP) was comparable to that formed in the PUR scaffolds not incorporating rhBMP-2 (FR and SR negative controls). Representative histological sections of the FR + BMP scaffolds (Fig. 7) revealed a remarkably consistent and unique pattern of new bone and marrow surrounded by a ring of osteoid, large blood vessels, and osteoblasts (identified as cuboidal cells on the osteoid surface) within the pores of the PUR scaffolds. When compared to the other treatments, this highly ordered structure and organization of the bone and marrow provides additional qualitative evidence that the FR + BMP system may have enhanced bone regeneration and reconstitution of marrow. It is possible that resorption of new bone was important to allow infiltration of the new marrow; however, this was not assessed here.

The limitations of the collagen sponge delivery system have been recognized,[43] which has prompted considerable discussion and investigation of improved delivery systems for rhBMP-2.[13,23–25] For large critical-sized defects that cannot heal spontaneously, a burst release that recruits osteoprogenitor cells into the scaffold, followed by a sustained release that promotes osteoblastic differentiation has been suggested as the ideal release strategy for rhBMP-2.[23] However, whereas this concept of the ideal delivery system is generally accepted, few studies have systematically compared different release strategies, especially in more challenging bone defects.[23,25]

A sub-optimal delivery system does not exploit the full potential of the released growth factor, thereby requiring doses that substantially exceed the therapeutic level.[23] In the present study, we used 2 μg rhBMP-2 (47 μg cm^{-3}), which is relatively close to the lower limit of the osteogenic threshold in rodents (13 μg cm^{-3}). Delivering doses greater than 2 μg of rhBMP-2 on a collagen sponge has been shown to dramatically increase the amount of bone in a very similar rodent model,[44] where 5 and 10 μg rhBMP-2 produced 48 and 91% more bone than the 2 μg dose, respectively. At the relatively low dose of 2 μg, the effects of pharmacokinetics on bone formation may be more distinct. In the present study, the combined burst and sustained release achieved with the FR + BMP scaffolds was more effective than the collagen sponge at the relatively low dose of rhBMP-2 investigated, thereby suggesting that the FR + BMP scaffold is a more efficient delivery system. Hence, the PUR scaffold approach may reduce the dose, and therefore the associated safety concerns and cost that is required to maximize the benefits of rhBMP-2 in patients.[8]

Both the physical properties and pharmacokinetics of the FR + BMP scaffold are believed to contribute to its superior performance compared to the collagen sponge delivery system. Key properties of the scaffold include high porosity, interconnected pores >100 μm that support cellular infiltration and mass transfer, high surface-to-volume ratio,[23] and controlled degradation to nontoxic breakdown properties. The PUR scaffolds investigated in this study exhibit these key physical properties.[28] Further, the observation of regenerated bone grown in direct contact with the PUR scaffold, even in the absence of rhBMP-2, suggests it is also osteoconductive and highly compatible for bone tissue engineering. Finally, the need to maintain defect volume is important in many clinical applications. As shown in Figure 4D, the resilient elastomeric mechanical properties of PUR scaffolds provided significantly improved space mainte-

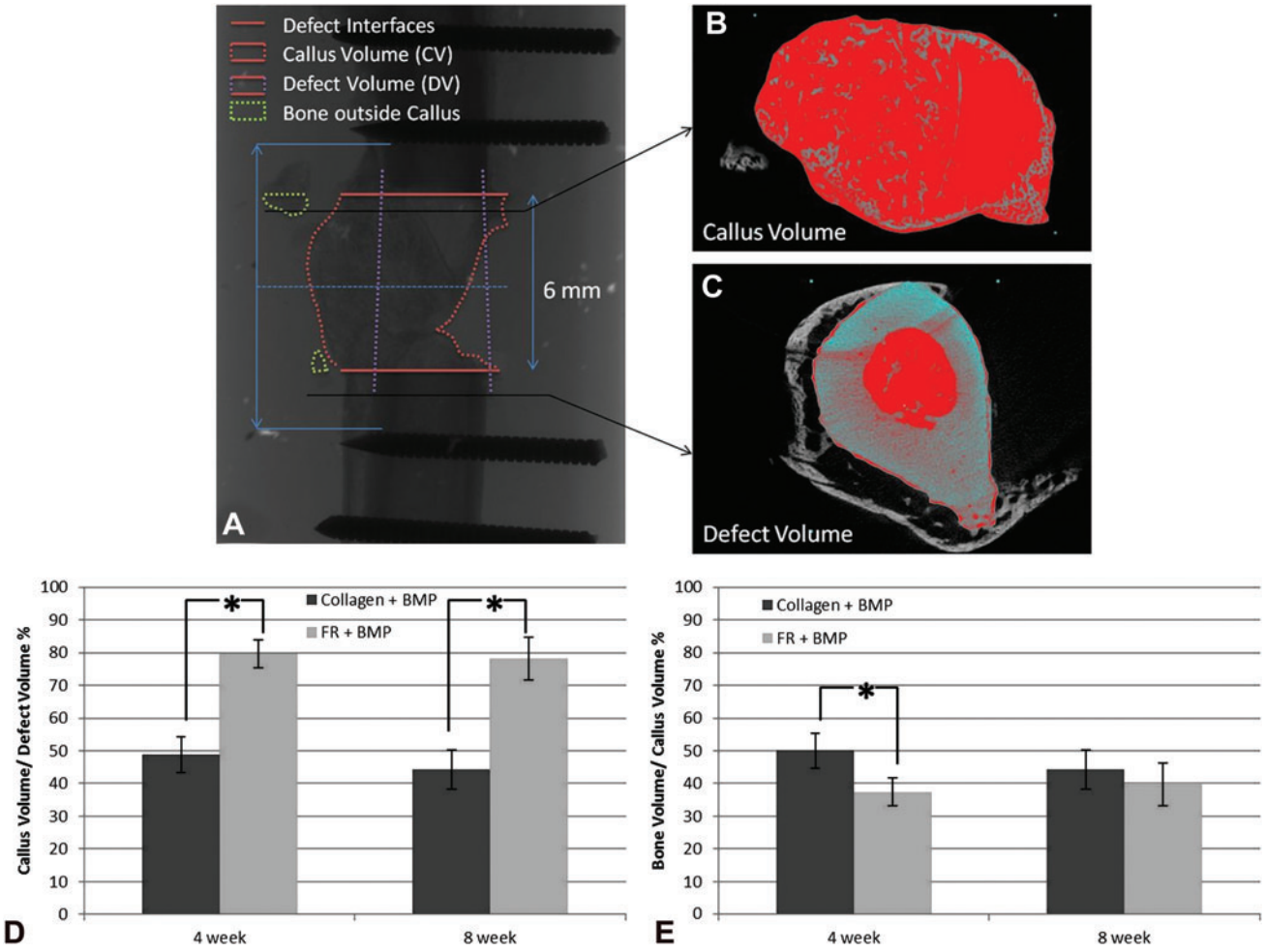

FIG. 4. **(A)** Schematic showing how the defect volume was analyzed from microCT images by distinguishing **(B)** callus volume region and **(C)** bone defect region. Comparison of **(D)** ossified callus space maintenance and **(E)** bone volume within the callus between the collagen + BMP and FR + BMP groups at 4 and 8 weeks. $*p < 0.01$. Color images available online at www.liebertonline.com/tea

nance compared to the collagen sponge (>78% for PUR scaffolds compared to <50% for the collagen scaffolds) at both 4 and 8 weeks ($p < 0.001$). This observation is in agreement with previous studies reporting that the collagen sponge lacks sufficient structural integrity to prevent soft tissue from prolapsing into the defect site.[45,46]

To effectively enhance bone regeneration, the release of rhBMP-2 must be localized to the defect site as well as regulated.[25] While the release of rhBMP-2 from the collagen sponge is adsorption controlled,[43] release of rhBMP-2 from PUR scaffolds is diffusion controlled,[27,29,37] and the pharmacokinetics can be modified by encapsulating the growth factor in microspheres of varying size.[37] The FR + BMP scaffold exhibited a biphasic release wherein 58% of the growth factor was released up to day 4 and an additional 13% released from days 5 to 21, which was the last time point measured. In contrast, the collagen sponge showed a bolus release, wherein 92% of the rhBMP-2 was released on day 1 and 100% on day 2 under *in vitro* conditions. Under *in vivo* conditions the release of rhBMP-2 from the collagen sponge has been reported to be more sustained, exhibiting a burst release followed by a sustained release until day 14.[23,47] The absence of *in vivo* pharmacokinetics data for collagen + BMP and FR + BMP limits the interpretation of the effects of the release profile on bone regeneration. However, the *in vitro* data suggest that the more sustained release from FR + BMP scaffolds for up to 3 weeks contributes to improved regeneration. This observation is consistent with previous studies demonstrating that rhBMP-2 available at later time points enhances bone regeneration due to additional osteoprogenitor cells at the fracture site at later timepoints.[19–21]

Surprisingly, there was not significantly greater new bone area at 8 weeks compared to 4 weeks within the treatment groups. Interestingly, whereas the volume of new bone did not significantly increase with time, 4 of the 10 of the FR + BMP scaffolds showed extensive formation of periosteal new bone that bridged the host cortices (Fig. 8) at 8 weeks, compared to only 1 of the 10 collagen + BMP sponges. This pattern of periosteal callus formation is consistent with the process of fracture healing, wherein osseous tissue replaces cartilage via endochondral ossification of a hypertrophic callus,[48] although mechanical testing is needed to specifically address the functional consequences of this observation. By 4 weeks the collagen sponge had completely degraded, resulting in complete release of rhBMP-2. Hence, there was no exogenous stimulus for more bone formation. In contrast, the

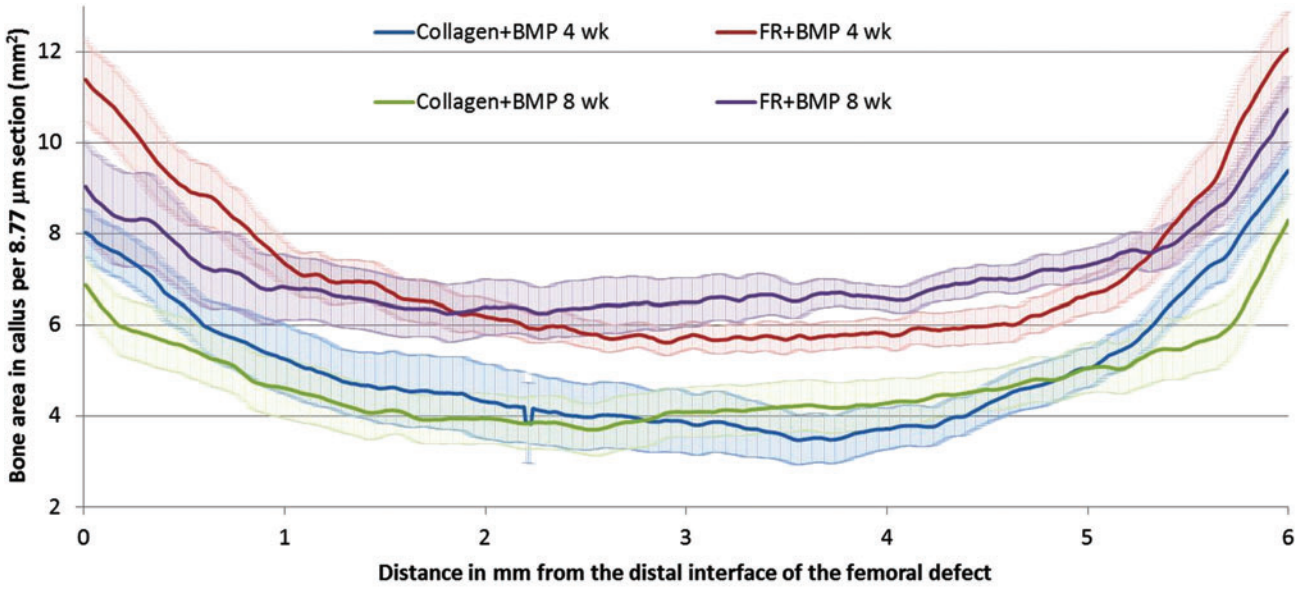

FIG. 5. Regenerated bone area in each 8.77 µm cross section of the defect from the distal to the proximal interface showing the FR + BMP group leads to greater bone regeneration at every location compared to the collagen + BMP group at both 4 and 8 weeks. Color images available online at www.liebertonline.com/tea

scaffold pores in the FR + BMP materials were fully infiltrated with bone, vasculature, and an apparently mature marrow at 4 weeks. The rate of polymer degradation (Fig. 9B) in the FR + BMP scaffolds was slow, decreasing from 51% of the total area at week 4 to 46% at week 8, which was not a significant difference. Thus, the rates of polymer degradation and anticipated bone regeneration are not matched, which likely hinders the rate of new bone formation.[23]

The polymer degradation data contrast with our previous study investigating the effects of recombinant human platelet-

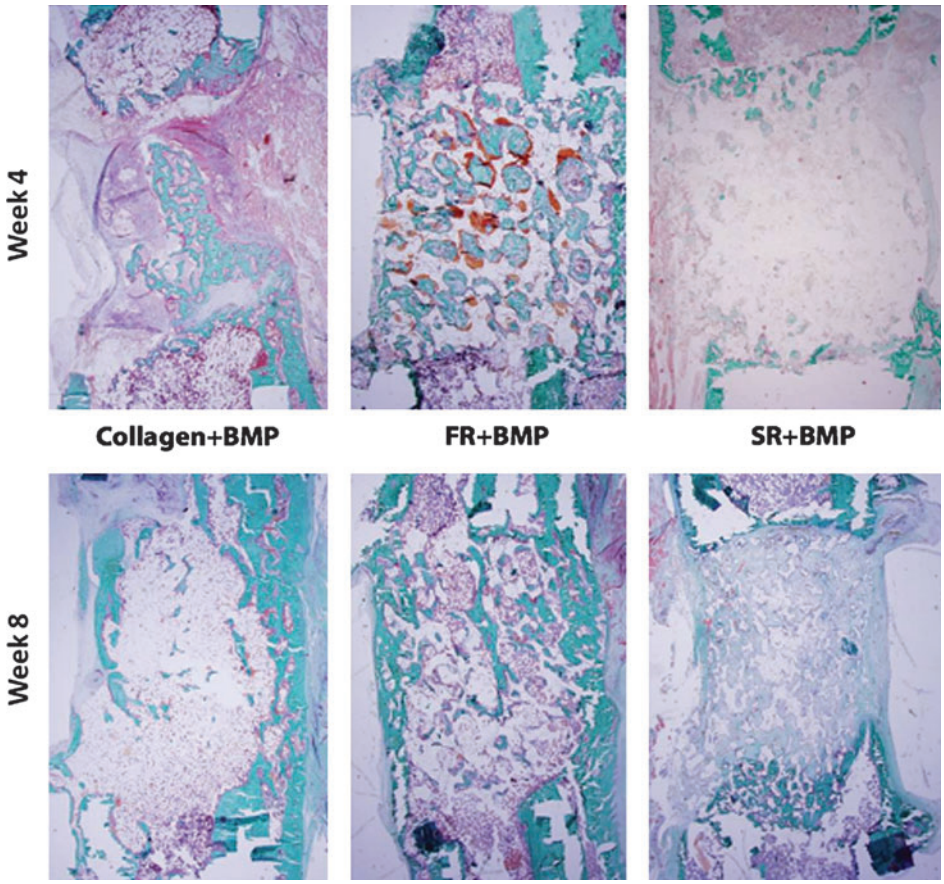

FIG. 6. Representative histological sections at low magnification (1.25×) showing cellular infiltration and new bone formation in collagen + BMP, FR + BMP, and SR + BMP. Color images available online at www.liebertonline.com/tea

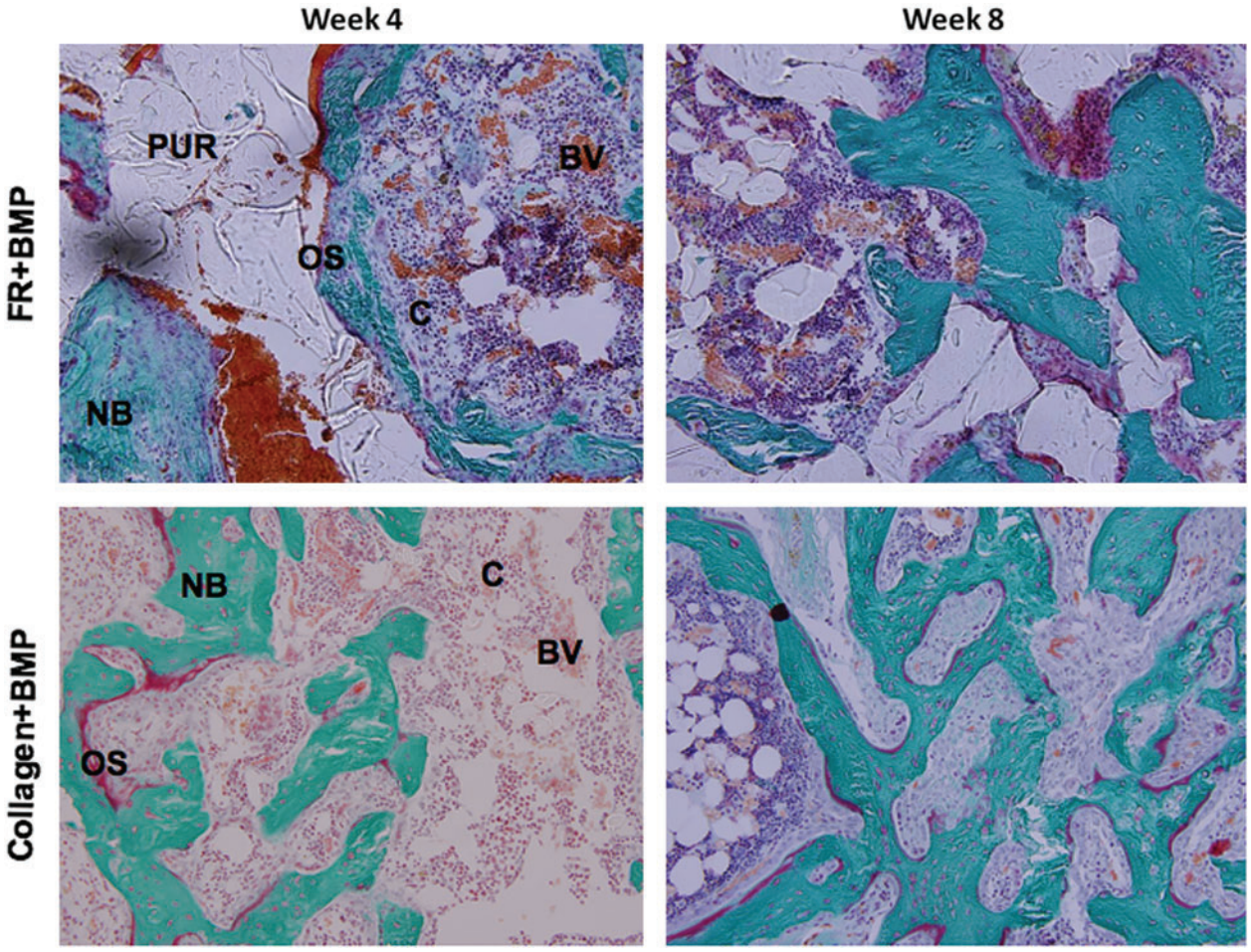

FIG. 7. Representative histological sections of collagen + BMP and FR + BMP treatment groups at high magnification (20×) showing osteoprogenitor cells (C), blood vessels (BV), osteoid (OS), new bone formation (NB), and residual polyurethane (PUR) scaffold. Color images available online at www.liebertonline.com/tea

derived growth factor (rhPDGF) delivered from PUR scaffolds on healing of excisional wounds in rats.[27] In the absence of rhPDGF, the amount of polymer decreased from 55% on day 3 to 25% on day 14. rhPDGF delivered from the scaffolds accelerated polymer degradation, as evidenced by the decrease in polymer fraction from 40% on day 3 to 5% on day 14. The accelerated degradation was attributed to enhanced recruitment of macrophages,[27] which secrete reactive oxygen

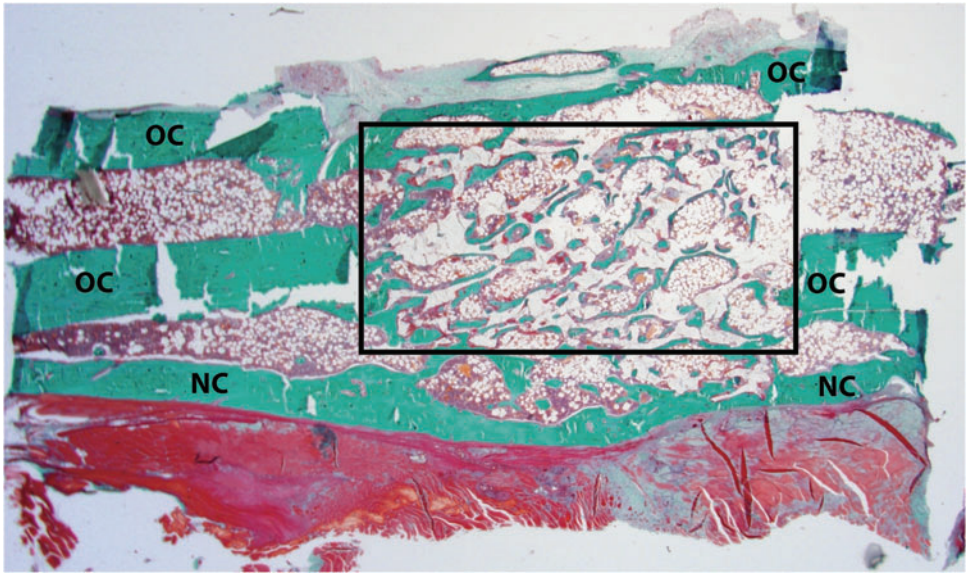

FIG. 8. Representative histological section at low magnification (1.25×) showing callus formation in FR + BMP scaffolds at 8 weeks. OC, original cortex; NC, new cortex. The box denotes the approximate boundary of the scaffold implanted in the defect site. Color images available online at www.liebertonline.com/tea

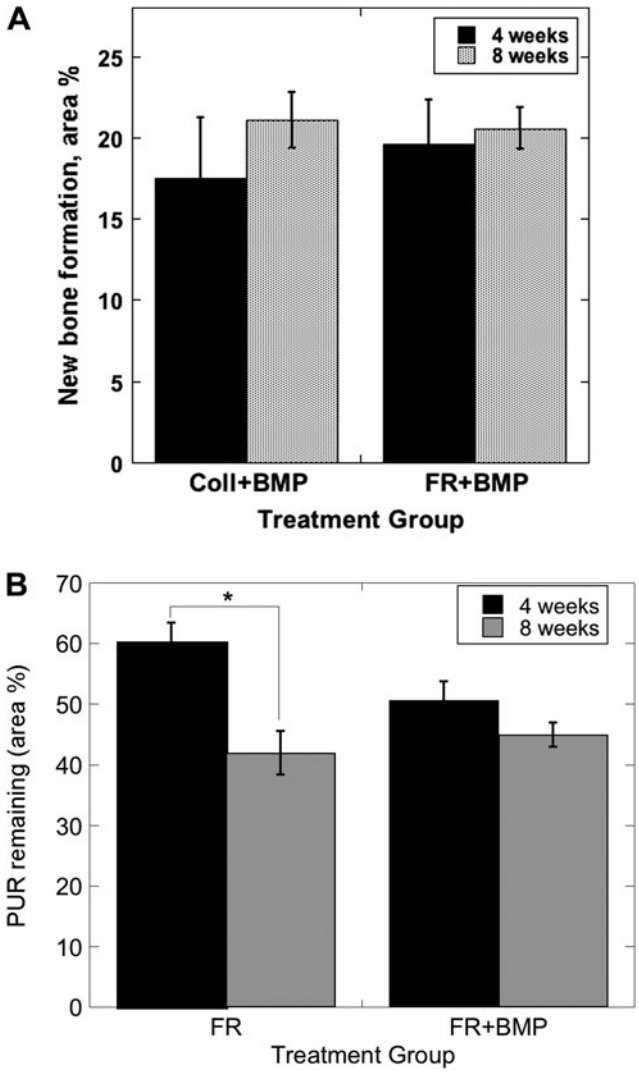

FIG. 9. Histomorphometric analysis. **(A)** New bone formation measured for collagen + BMP and FR + BMP. **(B)** Residual PUR measured for FR + BMP and FR scaffolds. *Significant differences ($p < 0.002$).

species (ROS) that actively degrade lysine-derived PURs.[49] However, in the present study, there was no evidence of cell-mediated degradation of the scaffold, and the rate of degradation approximated the *in vitro* hydrolytic rate.[28]

The SR + BMP scaffolds characterized by a sustained release of rhBMP-2 with no burst did not yield significantly more bone than either the SR or FR negative controls (Fig. 2A). The absence of significant new bone formation in SR + BMP scaffolds was surprising, considering our previous study showing that SR + BMP scaffolds promoted significantly more bone formation relative to the PUR scaffold without rhBMP-2.[37] This and other studies[50] show that PLGA is an effective delivery system for rhBMP-2, and that the inability of the SR + BMP scaffolds to promote bone formation in the present study cannot be attributed to adverse interactions between PLGA and rhBMP-2. Encapsulation of rhBMP-2 in 1.3 μm PLGA microspheres eliminated the burst release of rhBMP-2 from SR + BMP scaffolds,[37] thereby reducing the chemoattractant stimulus[23] that recruits osteoprogenitor cells into the scaffold. In another study investigating bone formation in 6-mm critical-sized rat femoral segmental defects, a linear release of rhBMP-2 exhibiting no burst (50% release after 21 days) promoted robust new bone formation at a dose of 6.6 μg, compared to 2.5 μg for the present study.[51,52] Thus, the combination of the negligible burst release and the low dose of rhBMP-2 was the likely reason for failure of the SR + BMP scaffolds to promote bone formation in the present study. In contrast, we have previously shown that SR + BMP scaffolds formed significantly more new bone than the SR scaffold when implanted in a rat femoral condyle plug defect.[37] Hence, the anatomic site may significantly impact the preferred release profile,[23] suggesting that caution should be used when extrapolating results across different animal models and anatomical sites. Moreover, higher doses of rhBMP-2 mask differences in bone regeneration observed for different release profiles.

Injectable biomaterials are of interest in orthopedics due to their potential for use in minimally invasive surgical procedures. A recent review has noted that injectable biomaterials generally do not possess a defined pore structure, which limits their effectiveness due to the reduction in tissue ingrowth.[53] Advantages of the PUR scaffolds investigated in this study include their injectability and the distinct ability to form pores with the desired size distribution through the gas foaming reaction *in situ*. We have previously shown that porous composites comprising a two-component reactive PUR and allograft bone particles (~180 μm mean size) injected into femoral plug defects in rats supported rapid cellular infiltration and new bone formation as early as 3 weeks without additional growth factors.[35] Addition of rhBMP-2 as a labile powder to the injectable PUR composite is thus a potentially promising injectable delivery system that is under investigation in our laboratories.

Conclusion

A burst followed by a sustained release of rhBMP-2 from a biodegradable PUR scaffold regenerated 50% more new bone compared to a collagen sponge loaded with rhBMP-2 in a rat critical-sized femoral defect during the first 4 weeks. No differences in new bone formation were observed at 8 weeks. This study demonstrated that an improved release profile for rhBMP-2 can be achieved using PUR scaffolds, and that this enhanced pharmacokinetics regenerated more bone than the clinically available standard of care in a critical-sized defect in rat femora. The very slow rate of polymer degradation is believed to be responsible for the lack of increase in BV between 4 and 8 weeks in the FR + BMP scaffolds, though this requires future investigation. Strategies for increasing the rate of scaffold degradation while maintaining the desired release kinetics and scaffold characteristics are needed to fully realize the osteogenic potential of rhBMP-2.

Acknowledgments

The opinions or assertions contained herein are the private views of the authors and are not to be construed as official or as reflecting the views of the Department of the Army or the Department of Defense.

This study was funded in part by a Department of Defense Grant (Orthopaedic Extremity Trauma Research Program #W81XWH-07-1-0211).

Disclosure Statement

No competing financial interests exist.

References

1. Harris, A.M., Althausen, P.L., Kellam, J., Bosse, M.J., and Castillo, R. Complications following limb-threatening lower extremity trauma. J Orthop Trauma **23,** 1, 2009.
2. Seeherman, H., Li, R., Bouxsein, M., Kim, H., Li, X.J., Smith-Adaline, E.A., Aiolova, M., and Wozney, J.M. rhBMP-2/calcium phosphate matrix accelerates osteotomy-site healing in a nonhuman primate model at multiple treatment times and concentrations. J Bone Joint Surg **88-A,** 144, 2006.
3. Li, R.H., Bouxsein, M.L., Blake, C.A., D'Augusta, D., Kim, H., Li, X.L., Wozney, J.M., and Seeherman, H.J. rhBMP-2 injected ina calcium phospahte paste (alpha-BSM) accelerates healing in the rabbit ulnar osteotomy model. J Orthop Res **21,** 997, 2001.
4. Chen, X.Q., Kidder, L.S., and Lew, W.D. Osteogenic protein-1 induced bone formation in an infected segmental defect in the rat femur. J Orthopaedic Res **20,** 142, 2002.
5. Patel, Z.S., Young, S., Tabata, Y., Jansen, J.A., Wong, M.E., and Mikos, A.G. Dual delivery of an angiogenic and an osteogenic growth factor for bone regeneration in a critical size defect model. Bone **43,** 931, 2008.
6. Kempen, D.H., Kruyt, M.C., Lu, L., Wilson, C.E., Florschutz, A.V., Creemers, L.B., Yaszemski, M.J., and Dhert, W.J. Effect of autologous BMSCs seeding and BMP-2 delivery on ectopic bone formation in a microsphere/poly(propylene fumarate) composite. Tissue Eng Part A **15,** 587, 2009.
7. Swiontkowski, M.F., Aro, H.T., Donell, S., Esterhai, J.L., Goulet, J., Jones, A., Kregor, P.J., Nordsletten, L., Paiement, G., and Patel, A. Recombinant human bone morphogenetic protein-2 in open tibial fractures. A subgroup analysis of data combined from two prospective randomized studies. J Bone Joint Surg Am **88,** 1258, 2006.
8. Govender, S., Csimma, C., Genant, H.K., Valentin-Opran, A., Amit, Y., Arbel, R., Aro, H., Atar, D., Bishay, M., Borner, M.G., Chiron, P., Choong, P., Cinats, J., Courtenay, B., Feibel, R., Geulette, B., Gravel, C., Haas, N., Raschke, M., Hammacher, E., van der Velde, D., Hardy, P., Holt, M., Josten, C., Ketterl, R.L., Lindeque,B., Lob, G., Mathevon, H., McCoy, G., Marsh, D., Miller, R., Munting, E., Oevre, S., Nordsletten, L., Patel, A., Pohl, A., Rennie, W., Reynders, P., Rommens, P.M., Rondia, J., Rossouw, W.C., Daneel, P.J., Ruff, S., Rüter, A., Santavirta, S., Schildhauer, T,A,, Gekle, C., Schnettler, R., Segal, D., Seiler, H., Snowdowne, R.B., Stapert, J., Taglang, G., Verdonk, R., Vogels, L., Weckbach, A., Wentzensen, A., Wisniewski, T., and BESTT Study Group. Recombinant human bone morphogenetic protein-2 for treatment of open tibial fractures: a prospective, controlled, randomized study of four hundred and fifty patients. J Bone Joint Surg **84-A,** 2123, 2002.
9. Urist, M.R. Bone morphogenetic protein: the molecularization of the skeletal system. J Bone Min Res **12,** 343,1997.
10. Cheng, H., Jiang, W., Phillips, F.M., Haydon, R.C., Peng, Y., Zhou, L., Luu, H.H., An, N., Breyer, B., Vanichakarn, P., Szatkowski, J.P., Park, J.Y., and He, T.C. Osteogenic activity of the fourteen types of human bone morphogenetic proteins (BMPs). J Bone Joint Surg **85-A,** 1544, 2003.
11. Fiedler, J., Roderer, G., Gunther, K.P., and Brenner, R.E. BMP-2, BMP-4, and PDGF-bb stimulate chemotactic migration of primary human mesenchymal progenitor cells. J Cell Biochem **87,** 305, 2002.
12. Uludag, H., Gao, T., Porter, T., Friess, W., and Wozney, J. Delivery systems for BMPS: factors contributing to the protein retention at an application site. J Bone Joint Surg **83-A,** S128, 2001.
13. Seeherman, H., and Wozney, J.M. Delivery of bone morphogenetic proteins for orthopedic tissue regeneration. Cytokine Growth Factor Rev **16,** 329, 2005.
14. Cho, T.J., Gerstenfeld, L.C., and Einhorn, T.A. Differential temporal expression of members of the transforming growth factor beta superfamily during murine fracture healing. J Bone Miner Res **17,** 513, 2002.
15. Tagil, M., Jeppsson, C., Wang, J.S., and Aspenberg, P. No augmentation of morselized and impacted bone graft by OP-1 in a weight-bearing model. Acta Orthop Scand **74,** 742, 2003.
16. Kloen P. Commentary & Perspective on "Recombinant Human BMP-2 and Allograft Compared with Autogenous Bone Graft for Reconstruction of Diaphyseal Tibial Fractures with Cortical Defects" by Alan L. Jones, MD, *et al.* Available at www.ejbjs.org/Comments/2006/cp_jul06_kloen.dtl. 2006.
17. Kempen, D.H., Lu, L., Heijink, A., Hefferan, T.E., Creemers, L.B., Maran, A., Yaszemski, M.J., and Dhert, W.J. Effect of local sequential VEGF and BMP-2 delivery on ectopic and orthotopic bone regeneration. Biomaterials **30,** 2816, 2009.
18. Patel, Z.S., Young, S., Tabata, Y., Jansen, J.A., Wong, M.E., and Mikos, A.G. Dual delivery of an angiogenic and an osteogenic growth factor for bone regeneration in a critical size defect model. Bone **43,** 931, 2008.
19. Kempen, D.H., Kruyt, M.C., Lu, L., Wilson, C.E., Florschutz, A.V., Creemers, L.B., Yaszemski, M.J., and Dhert, W.J. Effect of autologous bone marrow stromal cell seeding and bone morphogenetic protein-2 delivery on ectopic bone formation in a microsphere/poly(propylene fumarate) composite. Tissue Eng Part A **15,** 587, 2009.
20. Kim, S.S., Gwak, S.J., and Kim, B.S. Orthotopic bone formation by implantation of apatite-coated poly(lactide-co-glycolide)/hydroxyapatite composite particulates and bone morphogenetic protein-2. J Biomed Mater Res A **87,** 245, 2008.
21. Jeon, O., Song, S.J., Yang, H.S., Bhang, S.H., Kang, S.W., Sung, M.A, Lee, J.H. and Kim, B.S. Long-term delivery enhances *in vivo* osteogenic efficacy of bone morphogenetic protein-2 compared to short-term delivery. Biochem Biophys Res Commun **369,** 774, 2008.
22. de Jesus Perez, V.A., Alastalo, T.P., Wu, J.C., Axelrod, J.D., Cooke, J.P., Amieva, M., and Rabinovitch, M. Bone morphogenetic protein 2 induces pulmonary angiogenesis via Wnt-beta-catenin and Wnt-RhoA-Rac1 pathways. J Cell Biol **184,** 83, 2009.
23. Li, R.H., and Wozney, J.M. Delivering on the promise of bone morphogenetic proteins. Trends Biotechnol **19,** 255, 2001.
24. Haidar, Z.S., Hamdy, R.C., and Tabrizian, M. Delivery of recombinant bone morphogenetic proteins for bone regeneration and repair. Part B: Delivery systems for BMPs in orthopaedic and craniofacial tissue engineering. Biotechnol Lett **31,** 1825, 2009.
25. Haidar, Z.S., Hamdy, R.C., and Tabrizian, M. Delivery of recombinant bone morphogenetic proteins for bone regeneration and repair. Part A: Current challenges in BMP delivery. Biotechnol Lett **31,** 1817, 2009.
26. Guan, J., Stankus, J.J., and Wagner, W.R. Biodegradable elastomeric scaffolds with basic fibroblast growth factor release. J Control Release **120,** 70, 2007.
27. Li, B., Davidson, J.M., and Guelcher, S.A. The effect of the local delivery of platelet-derived growth factor from reactive two-component polyurethane scaffolds on the healing in rat skin excisional wounds. Biomaterials **30,** 3486, 2009.

28. Hafeman, A., Li, B., Yoshii, T., Zienkiewicz, K., Davidson, J.M., and Guelcher, S.A. Injectable biodegradable polyurethane scaffolds with release of platelet-derived growth factor for tissue repair and regeneration. Pharm Res **25,** 2387, 2008.
29. Li, B., Brown, K.V., Wenke, J.C., and Guelcher, S.A. Sustained release of vancomycin from polyurethane scaffolds inhibits infection of bone wounds in a rat femoral segmental defect model. J Control Release **145,** 221, 2010
30. Hafeman, A.E., Zienkiewicz, K.J., Carney, E., Litzner, B., Stratton, C., Wenke, J.C., and Guelcher, S.A. Local delivery of tobramycin from injectable biodegradable polyurethane scaffolds. J Biomater Sci Polym Ed **21,** 95, 2010.
31. Zhang, J.Y., Beckman, E.J, Hu, J., Yuang, G.G., Agarwal, S., and Hollinger, J.O. Synthesis, biodegradability, and biocompatibility of lysine diisocyanate-glucose polymers. Tissue Eng **8,** 771, 2002.
32. Zhang J.Y., Beckman, E.J., Piesco, N.J., and Agarwal, S. A new peptide-based urethane polymer: synthesis, biodegradation, and potential to support cell growth *in vitro*. Biomaterials **21,** 1247, 2000.
33. Gorna, K., and Gogolewski, S. Biodegradable polyurethanes for implants. II. *In vitro* degradation and calcification of materials from poly(epsilon-caprolactone)-poly(ethylene oxide) diols and various chain extenders. J Biomed Mater Res **60,** 592, 2002.
34. Adhikari, R., Gunatillake, P.A., Griffiths, I., Tatai, L., Wickramaratna, M., Houshyar, S., Moore, T., Mayadunne, R.T., Field, J., McGee, M., and Carbone, T. Biodegradable injectable polyurethanes: synthesis and evaluation for orthopaedic applications. Biomaterials **29,** 3762, 2008.
35. Dumas, J.E., Zienkiewicz, K., Tanner, S.A., Prieto, E.M., Bhattacharyya, S., and Guelcher, S.A. Synthesis and characterization of an injectable allograft bone/polymer composite bone void filler with tunable mechanical properties. Tissue Eng Part A **16,** 2505, 2010
36. Guelcher, S., Srinivasan, A., Hafeman, A., Gallagher, K., Doctor, J., Khetan, S., McBride, S., and Hollinger, J. Synthesis, *In vitro* degradation, and mechanical properties of two-component poly(ester urethane)urea scaffolds: effects of water and polyol composition. Tissue Eng **13,** 2321, 2007.
37. Li, B., Yoshii, T., Hafeman, A.E., Nyman, J.S., Wenke, J.C., and Guelcher, S.A. The effects of rhBMP-2 released from biodegradable polyurethane/microsphere composite scaffolds on new bone formation in rat femora. Biomaterials **30,** 6768, 2009.
38. Talwar, R., Di Silvio, L., Hughes, F.J., and King, G.N. Effects of carrier release kinetics on bone morphogenetic protein-2-induced periodontal regeneration *in vivo*. J Clin Periodontol **28,** 340, 2001.
39. Arosarena, O.A., and Collins, W.L. Defect repair in the rat mandible with bone morphogenic protein 5 and prostaglandin E1. Arch Otolaryngol Head Neck Surg **129,** 1125, 2003.
40. Morgan, E.F., Mason, Z.D., Chien, K.B., Pfeiffer, A.J., Barnes, G.L., Einhorn, T.A., and Gerstenfeld, L.C. Micro-computed tomography assessment of fracture healing: relationships among callus structure, composition, and mechanical function. Bone **44,** 335, 2009.
41. Suva, L.J., Seedor, J.G., Endo, N., Quartuccio, H.A., Thompson, D.D., Bab, I., and Rodan. G.A. Pattern of gene expression following rat tibial marrow ablation. J Bone Miner Res **8,** 379, 1993.
42. Willie, B.M., Petersen, A., Schmidt-Bleek, K., Cipitria, A., Mehta, M., Strube, P., Lienau, J., Wildemann, B., Fratzl, P., and Duda, G. Designing biomimetic scaffolds for bone regeneration: why aim for a copy of mature tissue properties if nature uses a different approach? Soft Mater **6,** 4976, 2010.
43. Luginbuehl, V., Meinel, L., Merkle, H.P., and Gander, B. Localized delivery of growth factors for bone repair. Eur J Pharm Biopharm **58,** 197, 2004.
44. Morishita, Y., Naito, M., Miyazaki, M., He, W., Wu, G, Wei, F., Sintuu, C., Hymanson, H., Brochmann, E.J., Murray, S.S., and Wang, J.C. Enhanced effects of BMP-binding peptide combined with recombinant human BMP-2 on the healing of a rodent segmental femoral defect. J Orthop Res **28,** 258, 2010.
45. Herford, A.S., and Boyne, P.J. Reconstruction of mandibular continuity defects with bone morphogenetic protein-2 (rhBMP-2). J Oral Maxillofac Surg **66,** 616, 2008.
46. Carter, T.G., Brar, P.S., Tolas, A., and Beirne, O.R. Off-label use of recombinant human bone morphogenetic protein-2 (rhBMP-2) for reconstruction of mandibular bone defects in humans. J Oral Maxillofac Surg **66,** 1417, 2008.
47. Winn, S.R., Uludag, H., and Hollinger, J.O. Sustained release emphasizing recombinant human bone morphogenetic protein-2. Adv Drug Deliv Rev **31,** 303, 1998.
48. Bailon-Plaza, A., and van der Meulen, M.C. A mathematical framework to study the effects of growth factor influences on fracture healing. J Theor Biol **212,** 191, 2001.
49. Hafeman, A.E., Zienkiewicz, K.J., Zachman, A.L., Sung, H.J., Nanney, L.B., Davidson, J.M., and Guelcher, S.A. Characterization of the degradation mechanisms of lysine-derived aliphatic poly(ester urethane) scaffolds. Biomaterials **32,** 419, 2011.
50. Jeon, O., Song, S.J., Kang, S.W., Putnam, A.J., and Kim, B.S. Enhancement of ectopic bone formation by bone morphogenetic protein-2 released from a heparin-conjugated poly(L-lactic-co-glycolic acid) scaffold. Biomaterials **28,** 2763, 2007.
51. Kempen, D.H., Lu, L., Heijink, A., Hefferan, T.E., Creemers, L.B., Maran, A., Yaszemski, M.J., and Dhert, W.J. Effect of local sequential VEGF and BMP-2 delivery on ectopic and orthotopic bone regeneration. Biomaterials **30,** 2816, 2009.
52. Kempen, D.H., Lu, L., Hefferan, T.E., Creemers, L.B., Maran, A., Classic, K.L., Dhert, W.J., and Yaszemski, M.J. Retention of *in vitro* and *in vivo* BMP-2 bioactivities in sustained delivery vehicles for bone tissue engineering. Biomaterials **29,** 3245, 2008.
53. Khan, Y., Yaszemski, M.J., Mikos, A.G., and Laurencin, C.T. Tissue engineering of bone: material and matrix considerations. J Bone Joint Surg **90A,** S36, 2008.

Address correspondence to:
Scott A. Guelcher, Ph.D.
Department of Chemical and Biomolecular Engineering
Vanderbilt University
2301 Vanderbilt Pl.
VU Station B #351604
Nashville, TN 37235

E-mail: scott.guelcher@vanderbilt.edu

Joseph C. Wenke, Ph.D.
Extremity Trauma and Regenerative Medicine Task Area
United States Army Institute of Surgical Research
3400 Rawley E. Chambers Ave.
Fort Sam Houston
San Antonio, TX 78234

E-mail: joseph.wenke@us.army.mil

Received: July 29, 2010
Accepted: February 18, 2011
Online Publication Date: April 1, 2011